E15-2007-81

A. Krása[1,2,*], F. Křížek[1,2], A. Kugler[1], M. Majerle[1,2],
V. Wagner[1,2], J. Adam[1,3], M. I. Krivopustov[3],
V. M. Tsoupko-Sitnikov[3], W. Westmeier[4], I. Zhuk[5]

NEUTRON EMISSION IN THE SPALLATION REACTIONS OF 1 GeV PROTONS ON A THICK LEAD TARGET SURROUNDED BY URANIUM BLANKET

[1]Nuclear Physics Institute ASCR PRI, Řež near Prague, Czech Republic
[2]Faculty of Nuclear Sciences and Physical Engineering, Czech Technical University in Prague, Czech Republic
[3]Joint Institute for Nuclear Research, Dubna, Russia
[4]Philipps-Universität, Marburg, Germany
[5]Joint Institute of Power and Nuclear Research, Sosny, Minsk, Belarus
[*]E-mail address: krasa@ujf.cas.cz

Краса А. и др. E15-2007-81
Эмиссия нейтронов в реакции скалывания
из массивной свинцовой мишени, окруженной
урановым бланкетом, под действием протонов с энергией 1 ГэВ

Толстая свинцовая мишень, окруженная урановым бланкетом, облучалась протонами с энергией 1 ГэВ. Возникающее нейтронное поле измерялось путем исследования пороговых реакций в активационных фольгах. Экспериментальные результаты сравниваются с расчетами по методу Монте-Карло в варианте MCNPX 2.6 C.

Работа выполнена в Лаборатории ядерных проблем им. В. П. Джелепова ОИЯИ.

Сообщение Объединенного института ядерных исследований. Дубна, 2007

Krása A. et al. E15-2007-81
Neutron Emission in the Spallation Reactions of 1 GeV
Protons on a Thick Lead Target Surrounded by Uranium Blanket

A thick lead target surrounded by uranium blanket was irradiated with 1 GeV protons. Measurement of the produced neutron field was performed by means of threshold reactions in activation foils. The experimental results were compared with Monte Carlo calculations performed with the MCNPX 2.6. C code.

The investigation has been performed at the Dzhelepov Laboratory of Nuclear Problems, JINR.

Communication of the Joint Institute for Nuclear Research. Dubna, 2007

INTRODUCTION

Within the framework of a complex research of Accelerator Driven Systems (ADS) [1], based on a subcritical nuclear reactor driven by an external spallation neutron source, several experiments were performed using the «Energy plus Transmutation» setup [2–6], which is composed of thick lead target and uranium blanket. The main aim of investigation on this setup is the transmutation of fission products and higher actinides by spallation neutrons. This paper describes measurement of spatial distribution of produced neutron field in the experiment performed on the proton beam with kinetic energy of 1 GeV.

These protons were directed to the Pb target. Intensive neutron fluxes were created in spallation reactions and then multiplied by fission inside the U blanket. Our interest was focused on the high-energy neutron component that was measured by threshold reactions on Al, Au, and Bi foils placed in front of, inside, and behind the target/blanket. The yields of β radioactive nuclei produced in activation reactions in these foils were determined by means of γ-spectroscopy (for more details see [3]).

Our main goal is to check the accuracy of the corresponding Monte Carlo simulations, which use various models of spallation reactions and cross-section libraries of neutron induced reactions. We use the MCNPX code that is able to simulate the course of spallation reactions and the propagation of high-energy neutrons through thick target. While investigations of this energy domain were not of high interest in the past because of their minor importance for classical light-water nuclear reactors, they will be important for ADS as well as for radioisotope protection issues in future high-energy facilities. Reliable predictions of the relevant physical processes strongly depend on the accuracy of available nuclear data.

1. ENERGY PLUS TRANSMUTATION (E+T) SETUP

The E+T setup is divided into four sections of 114 mm in length separated by 8 mm gaps, totally 480 mm. Each section is composed of a cylindrical Pb target (diameter of 84 mm) and a natural uranium blanket with a hexagonal cross section (side length of 130 mm). Each blanket section contains 30 uranium rods

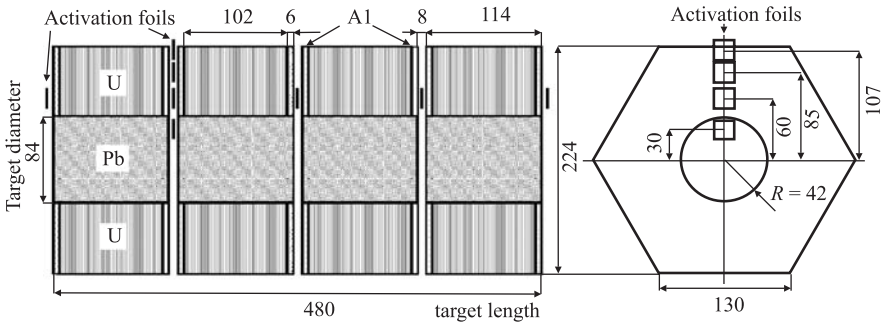

Fig. 1. The placement of activation foils: side view (left), cross-sectional view in the first gap (right). Dimensions are in millimeters

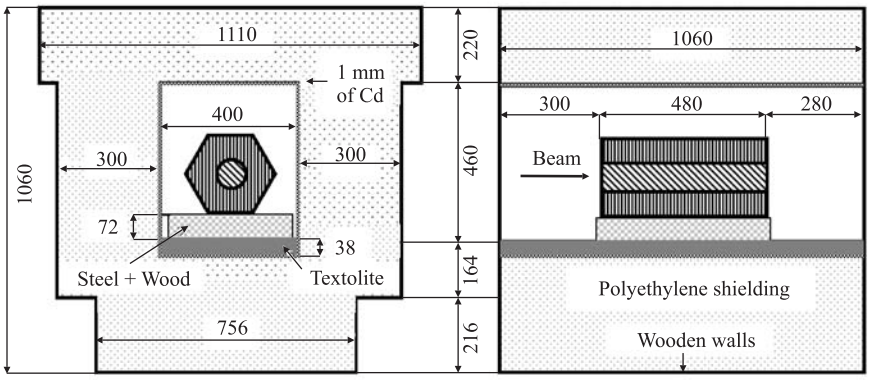

Fig. 2. Front view (left) and cross-sectional side view (right) of the «Energy plus Transmutation» setup. Dimensions are in millimeters

(diameter of 36 mm, length of 102 mm). There is totally 28.66 kg of $^{\mathrm{nat}}$Pb and 206.4 kg of $^{\mathrm{nat}}$U. The front and back ends of every blanket section are closed by aluminium plates of 6 mm in thickness (Fig. 1). The Pb target and the U rods are sealed in an aluminium cover of 2.0 mm and 1.27 mm in thickness, respectively (not pointed in Fig. 1).

This Pb/U-assembly is fixed on a wooden-metal rack ($362 \times 505 \times 72$ mm^3) and a textolite plate ($400 \times 1060 \times 38$ mm^3). The whole installation is placed in a polyethylene shielding (granulated $(CH_2)_n$, $\rho = 0.802$ g.cm^{-3}) of approximately cubic size ($1060 \times 1060 \times 1110$ mm^3) with walls from wood (Fig. 1). The inner walls of this container are coated with a Cd layer (thickness of 1 mm) used for absorption of thermal neutrons. The front and the back ends of the setup are

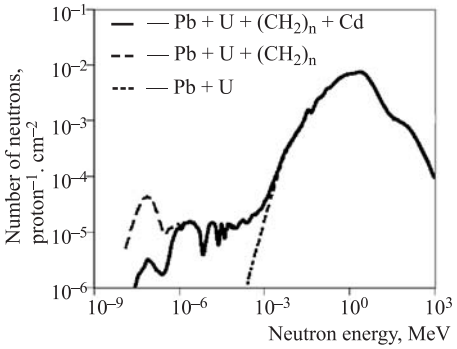

Fig. 3. Influence of the polyethylene shielding and the Cd layer on neutron spectra (MCNPX simulation of three different setups)

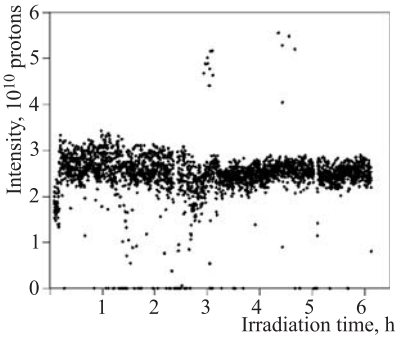

Fig. 4. The course of irradiation; each point represents one pulse of protons (measured by proportional chamber)

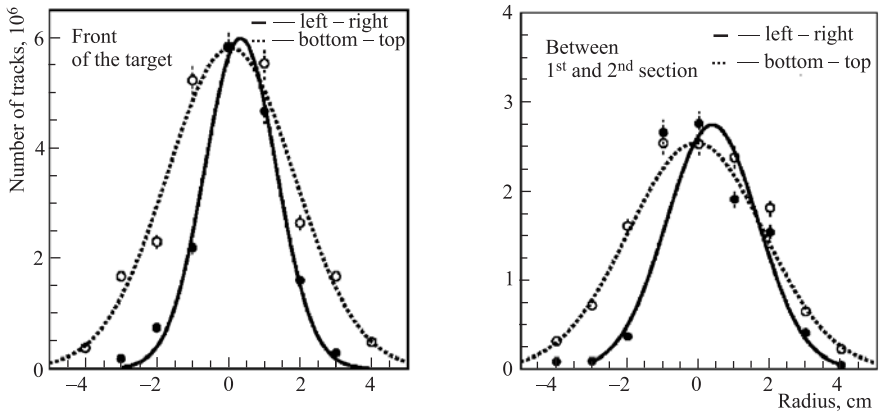

Fig. 5. Beam profile in front of the target (left) and in the first gap (right) fitted with Gaussian curve (measured by sets of SSNT detectors placed in two directions: from left to right and from bottom to top)

without shielding. The influence of individual setup components on produced neutron field was studied (Fig. 3), details are described in [8].

The E+T setup was irradiated with a 1 GeV proton beam for about six hours (Fig. 4). The accuracy of the beam energy was 0.5%. The total beam flux was measured by proportional chamber, Al and Cu activation foils. The beam geometry (shape, location, direction) was determined by lead solid state nuclear track (SSNT) detectors [7] and a set of Cu activation foils [3]. The central

Table 1. The parameters of 1 GeV proton beam

Irradiation time	Beam integral	Vertical FWHM	Horizontal FWHM	Vertical position	Horizontal position	Range (from [9])
6 h 03 min	$3.30(07) \cdot 10^{13}$	4.1(3) cm	2.4(3) cm	0.3(2) cm	0.3(2) cm	55 cm

part of beam profile was fitted by the Gaussian distribution (as the tails are not Gaussian) and we can conclude that the beam had approximately elliptical shape and was parallel with target axis (Fig. 1). The average beam parameters obtained independently by the above-mentioned methods see in Table 1.

2. EXPERIMENTAL RESULTS

The spatial distribution of the produced neutron field was measured by the Activation Analysis Method (AAM) using mono-isotopic foils from ^{27}Al, ^{197}Au, and ^{209}Bi. Al foils had square size of 20×20 mm^2 with thickness of 0.4 mm, Au foils had square size of 20×20 mm^2 with thickness of 0.04 mm, Bi foils had square size of 25×25 mm^2 with thickness of 1 mm.

The first set of activation foils (Al, Au, Bi) was placed at the radial distance $R = 6$ cm from the target axis at five *longitudinal* distances $X = 0.0; 11.8; 24.0; 36.2; 48.4$ cm from the target front (i. e., in front of the target, behind it, and in the gaps between blanket sections). The second set (only Al and Au) was placed in the first gap between the first and second blanket sections (i.e., at the longitudinal distance $X = 11.8$ cm from the target front) at four *radial* distances $R = 3.0; 6.0; 8.5; 10.7$ cm from the target axis. In sum, there were eight Al, eight Au (one foil belongs to both sets), and five Bi foils (Fig. 1).

Neutrons emitted in the course of spallation process in the target caused in the foils nonthreshold (n, γ) reaction and threshold (n, α), (n, xn) reactions. We observed the products of threshold reactions with $E_{\rm thresh}$ from 5 to 60 MeV, which correspond to x from 2 up to 9 (Tables 2, 3). The values of threshold energies were calculated as the difference between outgoing and incoming particle masses (using mass excesses values from [10]). In the case of the ^{27}Al$(n, \alpha)^{24}$Na reaction, the nuclear Coulomb barrier was taken into account and this $E_{\rm thresh}$ was estimated from [11].

The yields (i. e., the numbers of activated nuclei per one gram of foil material and per one incident proton) of observed isotopes are shown in the semi-logarithmic scale in Fig. 6. The delineated errors are only of statistical origin (given by the error of the Gaussian fit of the relevant γ peaks). Experimental errors, mainly the inaccuracies of the beam displacement, beam intensity, and γ-spectrometer efficiency determinations, contribute about 15%.

Table 2. The experimental yields of nuclei produced in Al and Au foils

Foil	^{27}Al	^{197}Au					
Reaction	(n,α)	(n,γ)	$(n,2n)$	$(n,4n)$	$(n,5n)$	$(n,6n)$	$(n,7n)$
Product	^{24}Na	^{198}Au	^{196}Au	^{194}Au	^{193}Au	^{192}Au	^{191}Au
$E_{\rm thresh}$, MeV	5.5	—	8.1	23	30	39	46
$T_{1/2}$, h	15	65	148	38	18	5	3
X, cm	Longitudinal yields, $10^{-6}\cdot$g$^{-1}\cdot$ proton^{-1}						
0.0	2.31(4)	89.0(6)	4.37(6)	0.926(22)	0.57(8)	0.377(18)	0.13(4)
11.8	4.24(6)	121.4(8)	7.72(9)	2.12(5)	1.72(10)	1.10(3)	0.46(6)
24.0	2.46(4)	120.6(8)	4.22(8)	1.33(4)	1.02(12)	0.72(4)	0.44(6)
36.2	1.332(23)	87.4(6)	2.12(6)	0.71(3)	0.62(8)	0.411(23)	0.25(4)
48.4	0.439(10)	53.2(4)	0.75(3)	0.334(17)	0.29(7)	0.203(16)	0.11(3)
R, cm	Radial yields, $10^{-6}\cdot$g$^{-1}\cdot$ proton^{-1}						
3.0	12.86(14)	146.8(12)	20.17(17)	6.09(8)	5.86(27)	4.11(16)	1.88(19)
6.0	4.24(6)	121.4(8)	7.72(9)	2.12(5)	1.72(10)	1.10(3)	0.46(6)
8.5	2.15(4)	127.1(9)	3.89(7)	1.13(3)	0.89(13)	0.51(3)	0.27(5)
10.7	1.24(3)	143.6(9)	2.39(7)	0.70(3)	0.67(16)	0.330(22)	0.23(6)

Table 3. The experimental yields of nuclei produced in Bi foils

Foil	^{209}Bi					
Reaction	$(n,4n)$	$(n,5n)$	$(n,6n)$	$(n,7n)$	$(n,8n)$	$(n,9n)$
Product	^{206}Bi	^{205}Bi	^{204}Bi	^{203}Bi	^{202}Bi	^{201}Bi
$E_{\rm thresh}$, MeV	22	30	38	45	53	61
$T_{1/2}$, h	150	367	11	12	2	2
X, cm	Longitudinal yields, $10^{-6}\cdot$ g$^{-1}\cdot$proton^{-1}					
0.0	0.57765)	0.466(10)	0.405(9)	0.317(16)	0.324(6)	0.198(11)
11.8	2.311(18)	1.58(4)	0.993(9)	0.700(18)	0.630(10)	0.316(16)
24.0	1.601(18)	1.12(4)	0.753(12)	0.557(19)	0.512(7)	0.299(14)
36.2	0.775(11)	0.59(3)	0.385(5)	0.295(10)	0.269(5)	0.170(7)
48.4	0.364(9)	0.298(22)	0.205(4)	0.182(8)	0.169(3)	0.103(6)

The yields of threshold reactions appear to have common shapes.

• The *radial* distributions of the yields of all isotopes produced in threshold reactions decrease nearly exponentially with increasing perpendicular distance from the target (beam) axis.

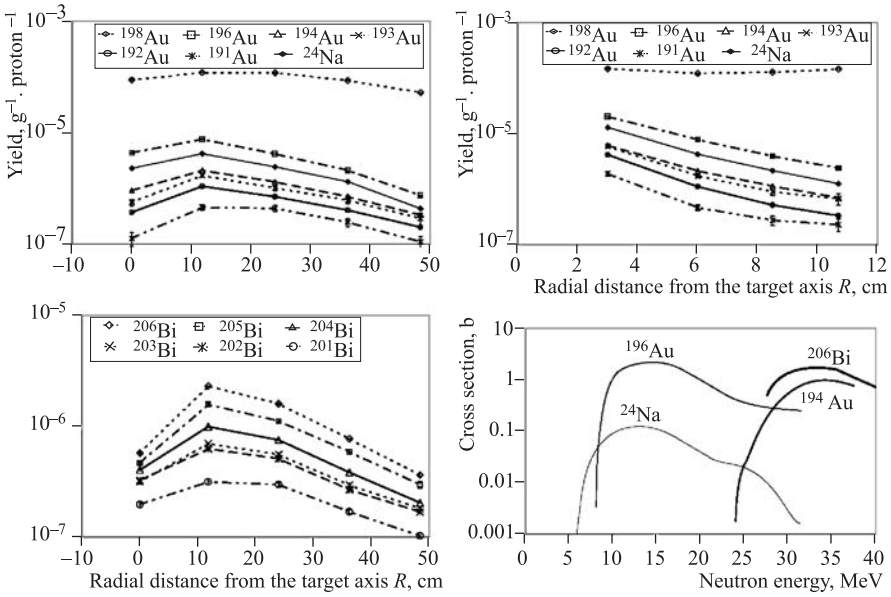

Fig. 6. Longitudinal (left) and radial (right) distributions of the experimental yields of nuclei produced in Al, Au, and Bi foils. The lines linking experimental points are delineated to guide the eyes. The plot below right shows examples of cross sections of observed reactions (fitted data for Al and Au [11], for Bi [12])

• The *longitudinal* distributions of the yields of all isotopes produced in threshold reactions change for one order of magnitude and have clear maximum observed in the first gap between blanket sections.

The yields of neutron capture show different shape.

• The *radial* distribution of ^{198}Au is almost constant. The reason for such a behaviour is the polyethylene shielding that moderates high-energy neutrons outgoing from the setup at first and then partly scatters low-energy neutrons back. Herewith, the moderator creates an intensive homogeneous field of low-energy neutrons (see Fig. 3) that is predominant in production of ^{198}Au. Therefore, the radial distribution of ^{198}Au is constant.

• The *longitudinal* distribution of ^{198}Au is mainly influenced by the polyethylene shielding as well. However, the contribution of low-energy neutrons from moderator is decreased in front of the target and behind it, because the target/blanket is not shielded from front and back ends (see Fig. 2). Therefore, the yields of ^{198}Au are lower in these positions.

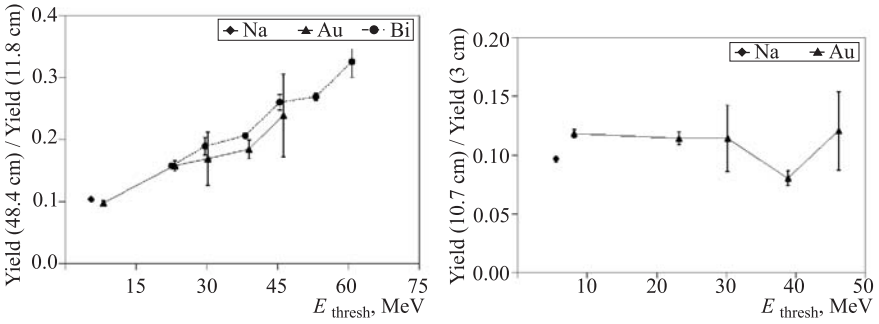

Fig. 7. Ratios of yields at the end of target (X = 48.4 cm) and inside the first gap (X = 11.8 cm) as a function of reaction threshold energy (left). Ratios of yields at R = 10.7 cm and at R = 3.0 cm as a function of reaction threshold energy (right). The lines link points belonging to one element

Ratios between yields at the end of target and in the first gap as a function of reaction threshold energy are shown in Fig. 7 (left). These ratios increase with increasing threshold energy. This indicates that the resulting neutron spectrum becomes harder at the end of the target than at its forepart.

Ratios between yields at R = 3.0 cm and at R = 10.7 cm as a function of reaction threshold energy are shown in Fig. 7 (right). In contrast to the latter, these ratios are not dependent on threshold energy. This is the sign that the shapes of fast neutron spectra are similar in both positions.

3. SIMULATIONS

The Monte Carlo simulations of neutron production in the E+T setup and of activation reactions in the foils were performed with the MCNPX code version 2.6. C [13, 14]. The influence of possible inaccuracies in the description of E+T setup geometry (in the MCNPX input file) on high-energy neutron component is negligible; low-energy neutron component is strongly influenced [8]. Following possibilities are available in MCNPX 2.6. C to describe spallation reaction:

• the intra-nuclear cascade (INC) of spallation reaction can be described with the Bertini INC model, Isabel INC model, Liège INC model, or CEM03 model (which works alone);

• the multistage pre-equilibrium exciton model (included in INC models) is the only model used for the pre-equilibrium emission of particles (only nucleons and charged pions were taken into account in our simulations);

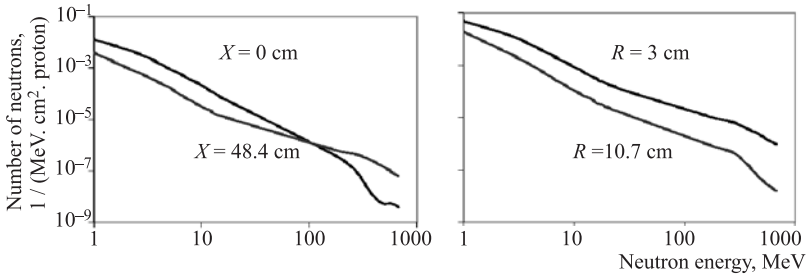

Fig. 8. Neutron spectra in front of ($X = 0$ cm) and behind ($X = 48.4$ cm) target (left). Neutron spectra inside target ($R = 3$ cm) and farther from target ($R = 10.7$ cm) (right). MCNPX simulation (Bertini+Dresner)

• the equilibrium emission of particles can be described with Dresner or ABLA evaporation models.

3.1. Neutron Spectra, Yields of Activation Reactions. At first, we have used the default option, i. e., Bertini+Dresner. The simulations of neutron flux show that the neutron spectrum is harder at the end of target when compared to its beginning and that the neutron spectrum has similar shape inside target as well as farther from it (Fig. 8). We drew the same conclusion from the experimental results (see Fig. 7).

The yields of nuclei produced in the activation foils were calculated directly with MCNPX and compared with experimental yields.

• The shapes of *longitudinal* distributions of yields are described well, see Fig. 9 (left). A quantitative agreement between experimental and simulated yields of threshold reactions is also good, the absolute differences are less than 30%. (The only exception is the first point for ^{206}Bi, where a problem appeared with the foil location and this value suffers from a significant systematic error.) About two times higher experimental yields than simulated ones were observed in the case of ^{198}Au. It is probably caused by not sufficiently precise description of setup shielding.

• In the cases of ^{196}Au and ^{194}Au, the ratios between experimental and simulated yields slightly grow with increasing *radial* distance from the target axis. This trend is a bit bigger for ^{194}Au. The shape of *radial* distribution of ^{24}Na is described very well. A quantitative agreement for all three isotopes is good, the absolute differences are less than 40%.

3.2. The Influence of Physics Models on Simulated Yields. As mentioned above, except the default description of spallation reaction by Bertini+Dresner, there are other INC+evaporation models available in MCNPX. The yields were calculated using all combinations of these models and compared with experimental yields. Figures 9 and 10 show following relations:

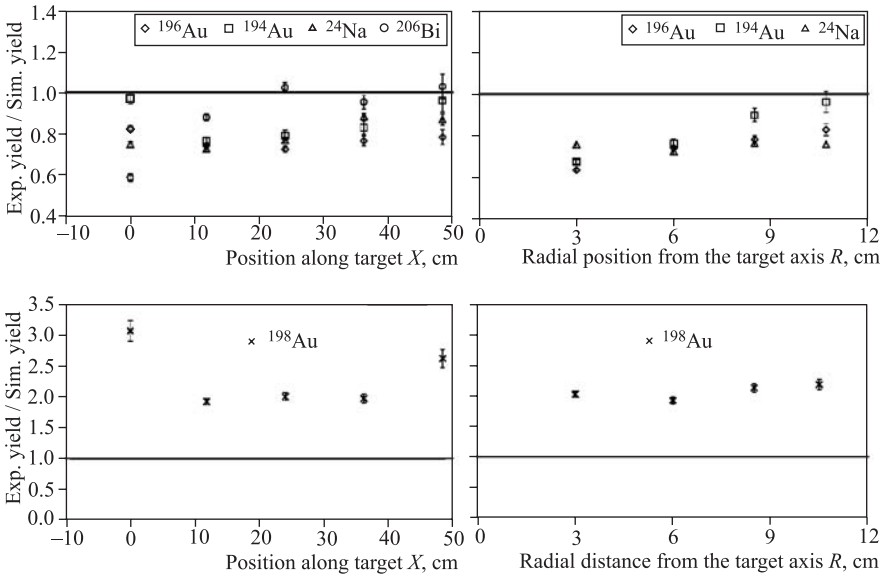

Fig. 9. The comparison of experimental and simulated (Bertini + Dresner) yields of isotopes produced in activation foils in longitudinal (left) and radial (right) directions

• ^{196}Au — simulation using Bertini+Dresner gives almost the same results as Isabel+Dresner; the same holds for Bertini+ABLA compared to Isabel+ABLA;

• ^{194}Au and ^{206}Bi — simulation using Bertini+Dresner gives almost the same results as Bertini + ABLA; the same holds for Isabel+Dresner compared to Isabel + ABLA.

Taking into account threshold energies and cross sections (see Tables 2, 3, and Fig. 2, below right), we conclude that evaporation models (Dresner and ABLA) have dominant influence for neutron energies up to $\simeq 25$ MeV. The INC models (Bertini and Isabel, which also include the pre-equilibrium model) are dominant for higher energies. This is not valid for the Liège INC model that has considerable influence on the evaporation part of neutron spectra.

Anyway, the simulations using combinations of all available physics models show approximately the same trends as the Bertini+Dresner combination (Fig. 10). Absolute differences from experiment are up to 50%, whereas Liège+ Dresner seems to fit the best for ^{196}Au and ^{24}Na, CEM03 for ^{194}Au, Bertini+ Dresner for ^{206}Bi. However, the relative variances between various model combinations are up to 50%. Because of this fact, we decided to pay attention to agreement between experimental and simulated **shapes** in longitudinal and radial

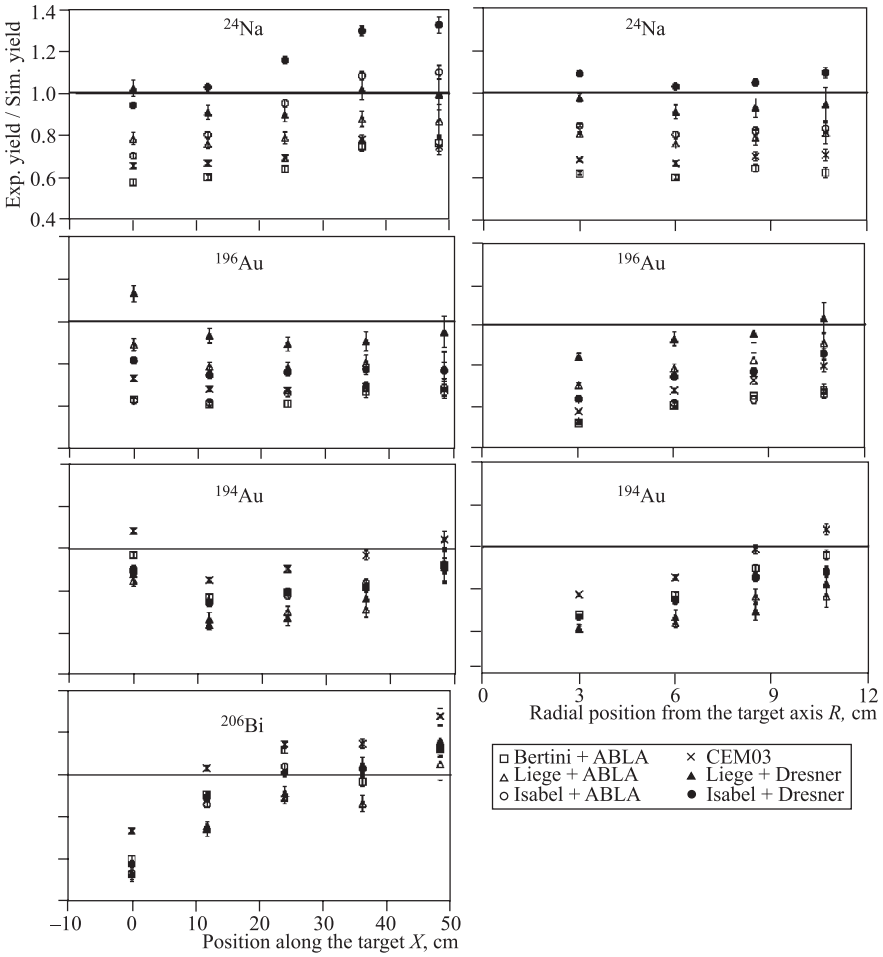

Fig. 10. The comparison of experiment with various combinations of INC+evaporation models. Longitudinal (left) and radial (right) distributions. Common legend is below right

distributions. Therefore, ratios for ^{196}Au, ^{194}Au, and ^{24}Na (from Fig. 9) were normalized to the the first foil in each set (Fig. 11). The shapes in longitudinal direction agree well, but slight discrepancy in radial direction shows systematic dependence on threshold energy, as mentioned above.

Similar trend was observed at the 1.5 GeV proton experiment, where the discrepancy between experimental and simulated values also increases with growing radial distance from the target axis, but much more strongly, even up to a

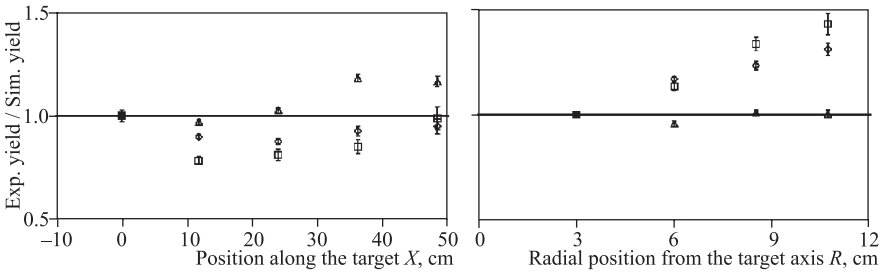

Fig. 11. The comparison of experimental and simulated (Bertini+Dresner) yields normalized to the first foil in each set

few times [2]. The detailed analysis of the experiments performed with proton beams (0.7, 1.0 (this paper), 1.5, 2.0 GeV [2]) and deuteron beams (1.6, 2.52 GeV [6]) could reveal the exact identification of the sources of differences observed between experimental data and simulations.

CONCLUSION

We studied high-energy neutron production in the spallation reactions of 1 GeV protons in the thick lead target with the uranium blanket surrounded by the polyethylene moderator. The shape and the intensity of produced neutron field were measured by means of threshold reactions in activation foils.

Due to the hard part of the neutron spectrum in the Pb/U-assembly, we observed isotopes produced in threshold reactions with $E_{\rm thresh}$ up to ~ 60 MeV. The maximum intensity of the fast neutron field ($E_n > 1$ MeV) produced in the spallation target was observed in the first gap between blanket sections. The energetic spectrum becomes harder at the end of the target.

The evaporation models (Dresner and ABLA) used in Monte Carlo simulations have dominant influence for neutron energies up to $\simeq 25$ MeV. The INC models (Bertini and Isabel) are dominant for higher energies.

MCNPX describes qualitatively well the shape of the *longitudinal* distributions of the yields of threshold reactions. Differences in absolute values are less than 50%. This is valid for all combinations of intra-nuclear cascade models with evaporation models included in the 2.6.C version. In contrast to the latter, the simulations predict a bit steeper decrease of yields with growing *radial* distance than was measured. This effect grows with the threshold energy. Similar trend, but much more distinctive, was observed at the 1.5 GeV experiment. Presently, we are not sure of the reason for this disagreement.

Acknowledgments. The authors thank to the LHE JINR for the possibility of using the Nuclotron accelerator for the experiments with the E+T setup and the Agency of Atomic Energy of Russia for supply of material for the uranium blanket. This work was carried out under the support of the GA CR (grant No. 202/03/H043) and GA AS CR (grant No. K2067107).

REFERENCES

1. *Brandt R. et al.* Accelerator driven systems for transmutation and energy production: challenges and dangers // Kerntechnik. 2004. V. 69. P. 37–50.

2. *Křížek F. et al.* The study of spallation reactions, neutron production and transport in a thick lead target and a uranium blanket during 1.5 GeV proton irradiation // Czech. J. Phys. 2006. V. 56. P. 243–252.

3. *Krása A. et al.* Neutron production in spallation reactions of 0.9 and 1.5 GeV protons on a thick lead target. Comparison between experimental data and Monte-Carlo simulations. JINR Preprint E1-2005-46. Dubna, 2005.

4. *Krivopustov M. I. et al.* First experiments with a large uranium blanket within the installation «Energy plus Transmutation» exposed to 1.5 GeV protons // Kerntechnik. 2003. V. 68. P. 48–54.

5. *Krivopustov M. I. et al.* Investigation of neutron spectra and transmutation of ^{129}I, ^{237}Np and other nuclides with 1.5 GeV protons from the Dubna Nuclotron using the electronuclear installation «Energy plus Transmutation». JINR Preprint E1-2004-79. Dubna, 2004.

6. *Krivopustov M. I. et al.* About the first experimental investigation of neutron production and transmutation of ^{129}I, ^{237}Np, ^{238}Pu, ^{239}Pu on Pb-target with U-blanket of «Energy plus Transmutation» setup irradiated by 2.52 GeV deuterons. JINR Preprint E1-2007-07. Dubna, 2007.

7. *Zhuk I. V. et al.* Investigation of energy-space distribution of neutrons in the lead target and uranium blanket within the installation «Energy plus Transmutation» exposed to 1.5 GeV protons. JINR Preprint P1-2002-184. Dubna, 2002.

8. *Majerle M. et al.* Setup consisting of a lead target and a uranium blanket as a tool for transport code testing (in press).

9. *Berger M. J. et al.* Stopping-power and range tables for electrons, protons, and helium ions (2005). [http://physics.nist.gov/PhysRefData/Star/Text/contents.html]

10. *Audi G. et al.* The NUBASE evaluation of nuclear and decay properties // Nucl. Phys. A. 2003. V. 729. P. 3–128.

11. *Uwamino Y. et al.* Measurement of neutron activation cross sections of energy up to 40 MeV using semimonoenergetic p–Be neutrons // Nucl. Sci. Eng. 1992. V. 111. P. 391.

12. *Kim E. et al.* Measurements of neutron spallation cross-sections of ^{12}C and ^{209}Bi in the 20- to 150 MeV energy range // Nucl. Sci. Eng. 1998. V. 129. P. 209.

13. *Pelowitz D. B. et al.* MCNPX Users's manual. Version 2.5.0. LANL report LA-CP-05-0369. 2005.

14. *Hendricks J. S. et al.* MCNPX, VERSION 2.6.C. LANL report LA-UR-06-7991. 2006.

Received on June 5, 2007.

Корректор *Т. Е. Попеко*

Подписано в печать 02.10.2007.
Формат 60 × 90/16. Бумага офсетная. Печать офсетная.
Усл. печ. л. 1,18. Уч.-изд. л. 1,67. Тираж 290 экз. Заказ № 55913.

Издательский отдел Объединенного института ядерных исследований
141980, г. Дубна, Московская обл., ул. Жолио-Кюри, 6.
E-mail: publish@jinr.ru
www.jinr.ru/publish/